Manufacture of Solid Oral Dosage Forms with Micro-structure Features via Rapid Tooling Injection Moulding

Erin Walsh[a,b], Elke Prasad[a,b], Joop H. ter Horst[a,b], Daniel Markl[a,b,*]

[a]*Strathclyde Institute of Pharmacy and Biomedical Sciences, University of Strathclyde, Glasgow, UK*
[b]*Future Continuous Manufacturing and Advanced Crystallisation Research Hub, University of Strathclyde, Glasgow, UK*

Abstract

With advancements in the pharmaceutical industry pushing more towards tailored medicines, novel approaches to tablet manufacture are in high demand. This study demonstrates the use of Rapid Tooling Injection Moulding (RTIM) as a tablet manufacture process. A number of polymeric formulations were trialled to produce three different tablet geometries. The surface area of these designs was altered while the volume was maintained, resulting in three different specific surface areas. Mass variability of the tablets produced was found to be low and well within pharmacopoeia limits. For the majority of the formulations tested the dimensions of the tablets produced were true to the digital design. The RTIM process has demonstrated its ability to produce tablets of defined specific surface area which is of particular interest for the modification of drug dissolution profiles.

Keywords: dissolution, injection moulding, rapid tooling, specific surface area, additive manufacture

1. Introduction

It is widely accepted that the pharmaceutical industry needs to be open to advancing and developing both current and novel technologies in order to continue to meet the demands and rigorous regulations within the industry (Goyanes et al., 2015). As the pharmaceutical industry steps away from traditional large scale industrial production and towards a more personalised approach to medicine the potential of novel manufacture

*Corresponding Author: daniel.markl@strath.ac.uk

techniques is clear (Alomari et al., 2015). One such technique is additive manufacture, commonly referred to as 3D printing. This technique has demonstrated its ability to produce tablets with differing geometries and has linked these to the drug release profiles produced (Goyanes et al., 2015; Karasulu and Ertan, 2002). This work aims to further expand on this area of research by combining both additive manufacture and injection moulding techniques as a method for tablet production. This process is known as Rapid Tooling Injection Moulding (RTIM).

The RTIM process utilises heat to encourage a thermoplastic material to adopt the desired geometry. Thermoplastics are a particularly large collection of materials which all have unique thermal, mechanical and electrical characteristics and therefore they do not all behave identically (Giboz et al., 2007; Heckele and Schomburg, 2004). The differing material properties of these thermoplastic materials therefore need to be understood to utilise them effectively in an RTIM process. Pressure-volume-temperature (PVT) behaviour, polymer structure and morphology and material crystallinity are all material properties that will have a major impact on the IM process (Annicchiarico and Alcock, 2014). The rheological behaviour of the polymer when molten or softened is particularly important in the RTIM process. Rheology is the study of material deformation under force (Satin and Bílik, 2016). Rheological characterisation of molten polymers is a commonly used analysis in process monitoring, quality control, process design and also in modelling and simulation (Zhang and Gilchrist, 2012). To understand the rheological behaviour of a material you can either observe how the material deforms under a given force, or determine the force required to achieve the desired deformation (Satin and Bílik, 2016). When studying material rheology, the first property to consider is whether the material acts as a Newtonian or a non-Newtonian fluid. The rheological behaviour of Newtonian fluids (linear elastic materials) is far simpler to understand and a general equation can be used to describe how these materials will react to deformation (Satin and Bílik, 2016). A constitutive equation or rheological equation of state can therefore be produced for Newtonian fluids which describes their flow (Satin and Bílik, 2016). Not all materials behave in this way and understanding the rheology of non-Newtonian fluids is far more complex. Molten thermoplastics are examples of non-Newtonian fluids and as such, they are rheologically complex and can exhibit interesting rheological properties

(Satin and Bílik, 2016). One of the major differences observed between Newtonian and non-Newtonian fluids is their viscosity. Viscosity is defined as shear stress divided by shear rate and this can be seen in Equation 1 from (Newton, 1687).

$$\tau = \eta \cdot \dot{\gamma} \rightarrow \eta = \frac{\tau}{\dot{\gamma}}[Pa \cdot s] = [\frac{Pa}{\frac{1}{s}}] \tag{1}$$

Where τ is the shear stress, η is the dynamic viscosity, $\dot{\gamma}$ is the shear rate, Pa is pressure and s is time in seconds.

For Newtonian fluids, viscosity is independent of time and only temperature, pressure and molecular properties of the material itself impact the speed shear deformation (Satin and Bílik, 2016). A number of process parameters involved in IM will therefore impact the viscosity of the thermoplastic material such as shear stress, shear rate, temperature and pressure. Non-newtonian injection materials demonstrate significant changes to their melt viscosity with relatively small variation in the shear rate making the prediction of process parameters difficult. This change in melt viscosity is due to the entanglement and disentanglement of polymer chains when the external forces of the injection moulding process are applied (shear) (Kashyap and Datta, 2015). Additionally, there is some evidence which suggests that the viscosity of molten thermoplastics is lower in the micro-channels of a μ-IM mould than is measured using a capillary rheometer (Zhang and Gilchrist, 2012). This is of particular importance for RTIM as the mould channels fall into this micro-range.

Material for IM is often prepared via hot melt extrusion (HME). HME is a technique used to combine materials to achieve sufficient mixing through the use of heating and shear stress. The viscosity of the molten mixtures is also important in the HME process. It must be low enough to not exceed the torque capability of the extruder but also must be sufficient to allow proper mixing (Verstraete et al., 2016). HME processing is typically possible with complex viscosity values between 1,000 and 10,000 Pa s (Verstraete et al., 2016). It is a fair assumption that a formulation that is processable by HME should also be processable by macro-IM, however a lower viscosity may be required for micro-IM techniques such as the RTIM involved in this work. Polymers which demonstrate good melt flow properties are typically preferred for RTIM. These materials typically have a low viscosity and include polypropylene (PP), polyethylene (PE), polyether ether ketone

(PEEK) and cyclic olefin copolymer (COC) (Packianather et al., 2015).

The objectives of this work are to develop a process for producing solid oral dosage forms (tablets) with micro-features designed to control specific surface area using the RTIM technique. Three different tablet geometries will be produced. These dosage forms will be comprised of pharmaceutical grade polymers (with the exception of one reference material) which are typically used in hot melt extrusion, injection moulding and additive manufacturing. The processability of a number of materials will be assessed as will the accuracy and precision of the process in reference to the digital design of the tablets.

2. Materials and Methods

2.1. Materials

2.1.1. Stereolithography Additive Manufacture

The photoresin used in this work is Clear v4 from Formlabs (Massachusetts, USA) based on the findings from (Walsh et al., 2021). Isopropyl alcohol (Sigma Aldrich, USA) is used to wash the moulds post-printing.

2.1.2. Rapid Tooling Injection Moulding

Raw Materials

A number of raw materials were used in this work. The names, supplier details and acronyms are detailed in Table 1. The acronym for each material will be used throughout this manuscript to refer to a particular material.

For a number of formulations, a aerosol silicone-based lubricant is required to aid removal from the mould (WD-40, USA).

Extrudates

A number of the formulations used in this work require preparation via hot melt extrusion. A series of formulations comprised solely of polymers or polymers with plasticising agents were produced and are detailed in Table 2. All formulation ratios are by weight.

Table 1: List of raw materials, their supplier details and their acronym codes that will be used in this manuscript.

Material	**Supplier**	**Acronym**
Affinisol HPMC HME 15LV	The Dow Chemical Company, USA	AFF
Eudragit E PO	Evonik, Germany	EPO
Klucel EF	Ashland, USA	KEF
Klucel ELF	Ashland, USA	KELF
Klucel LF	Ashland, USA	KLF
Low-density Polyethylene	Sigma Aldrich, USA	LDPE
Polyethylene	Sigma Aldrich, USA	PE
Polyethylene Glycol 4000	Sigma Aldrich, USA	PEG
Polyvinyl alcohol	Sigma Aldrich, USA	PVA
Soluplus®	BASF, Germany	SOL
Sorbitol Emprove Parteck SI 150	Merck, USA	SOR
Stearic Acid	Sigma Aldrich, USA	SA

2.2. Methods

2.2.1. Stereolithography Additive Manufacture

Mould inserts were printed using the Form 2 (Formlabs, Massachusetts) stereolithography (SLA) printer. The moulds are printed at a 45° angle from the build platform. On completion of printing, the moulds are washed in isopropyl alcohol in the agitated wash bath for a period of 10 minutes before being left to dry completely. The moulds are then removed from the build platform and placed in the FormCure for 60 minutes at 60 °C. Supporting material is removed and any surface roughness on the rear of the mould surface is lightly sanded. Further detail on the method used can be found in Walsh et al. (2021).

2.2.2. Design of Tablet Geometries

Three tablet geometries were produced for this study (see Figure 1). Conical frustrum shaped pins (see Figure 2b) are added to the designs in increasing number ($n = 2, 6$ or 10). In order to maintain the tablet mass across all three designs for a formulation,

Table 2: List of polymer-based formulations and their acronyms that will be used in this manuscript.

Primary Polymer	**Plasticiser**	**Prep Method**	**Acronym**
Affinisol	-	HME	AFF
Affinisol (85%)	Polyethylene Glycol (15%)	HME	AFF/PEG 85/15
Affinisol (85%)	Stearic acid (15%)	HME	AFF/SA 85/15
Affinisol (85%)	Polyethylene (15%)	HME	AFF/PE 85/15
Eudragit EPO (85%)	Polyethylene Glycol (15%)	HME	EPO/PEG 85/15
Klucel EF	-	HME	KEF
Klucel ELF	-	HME	KELF
Klucel LF	-	HME	KLF
LDPE	-	Pellets	LDPE
Polyvinyl Alcohol	-	HME	PVA
Soluplus (85%)	Sorbitol (15%)	HME	SOL/SOR 85/15

the volume of the three designs must be kept constant. In order to achieve this, the diameter of the tablets is adjusted to account for any change in volume resulting from the introduction of the pins. The thickness of each tablet is kept constant for all three designs as are the dimensions of each pin.

The surface area of the tablets is calculated using the following equation:

$$A_{tab} = 2\pi r_{cyl} h_{cyl} + 2\pi {r_{cyl}}^2 + n\pi \left[{r_{pin1}}^2 - {r_{pin2}}^2 + (r_{pin1} + r_{pin2}) \sqrt{(r_{pin1} - r_{pin2})^2 + {h_{pin}}^2} \right] \tag{2}$$

(3)

Where A_{tab} is the tablet surface area, r_{cyl} is the radius of the cylinder, h_{cyl} is the height of this cylinder, n is the number of pins, r_{pin1} is the top radius of the pin, r_{pin2} is the bottom radius of the pin and h_{pin} is the depth of the pin.

The volume of the tablets is calculated using the following equation:

$$V_{tab} = 2\pi {r_{cyl}}^2 h_{cyl} - \left(\frac{1}{3} \pi n h_{pin} \left({r_{pin1}}^2 + {r_{pin2}}^2 + r_{pin1} r_{pin2} \right) \right) \tag{4}$$

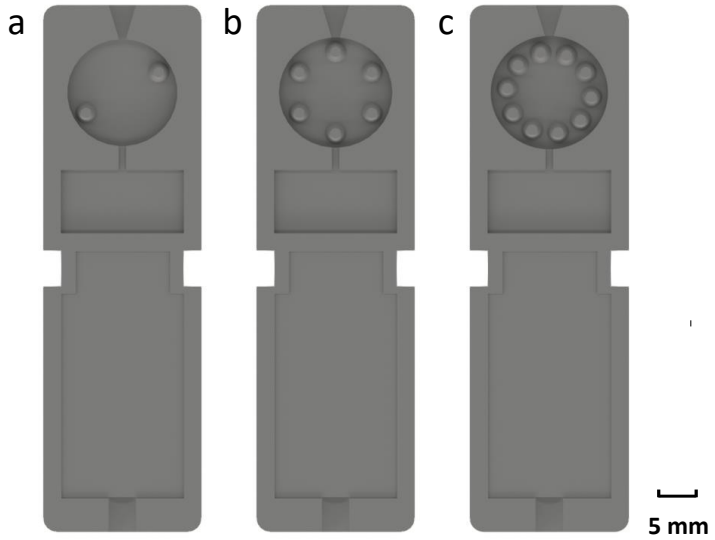

Figure 1: The three mould designs used in this study. a) 2 Pin b) 6 Pin c) 10 Pin.

Where V_{tab} is the tablet volume, r_{cyl} is the radius of the cylinder, h_{cyl} is the thickness of the cylinder, n is the number of pins, h_{pin} is the depth of the pin, r_{pin1} is the top radius of the pin and r_{pin2} is the bottom radius of the pin.

The specific surface area is calculated using:

$$SSA_{tab} = \frac{A}{V} \tag{5}$$

Full details of the tablet dimensions produced from these designs can be found in Table 3.

2.2.3. Rapid Tooling Injection Moulding

The Rapid Tooling Injection Moulding (RTIM) process couples SLA with Injection Moulding (IM). Mould inserts, produced via SLA, are housed within a metal mould casing (see Figure 3). Also visible are a number of design features on the printed mould insert to make it suitable for use in the RTIM process. The tablet cavity is the section of the mould insert which will produce the solid oral dosage form. The air cavity provides an overfill space for any excess injection material and offers a space for the air to compress upon moulding. The removal points can be found on each side of the mould, these aid in

Table 3: Summary table of tablet dimensions.

Design Feature	**2 Pin Design**	**6 Pin Design**	**10 Pin Design**
Diameter (mm)	15.23	15.69	16.12
Thickness (mm)	3	3	3
Volume (mm^3)	530.14	530.14	530.14
Surface Area (mm^2)	510.38	540.23	568.71
Number of Pins	2	6	10
Pin Depth (mm)	2	2	2
Pin Radius 1 (mm)	1.5	1.5	1.5
Pin Radius 2 (mm)	0.75	0.75	0.75
Specific Surface Area (mm^2/mm^3)	1.0	1.12	1.24

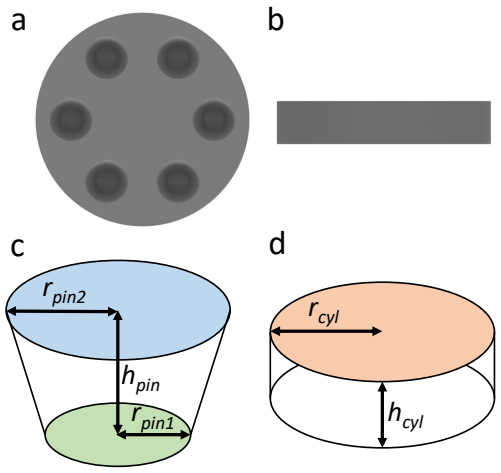

Figure 2: L: A rendering of the tablet design produced by the 6 Pin Design R: A close-up of the pins including details of the radii.

removing the mould inserts from the metal moulds. The separation point at the bottom of the mould inserts is used to separate the two halves of the mould insert.

The two halves of the metal mould were pieced together and placed into the HAAKE MiniJet Pro Piston Injection Moulding System (Thermo Fisher Scientific, USA) which

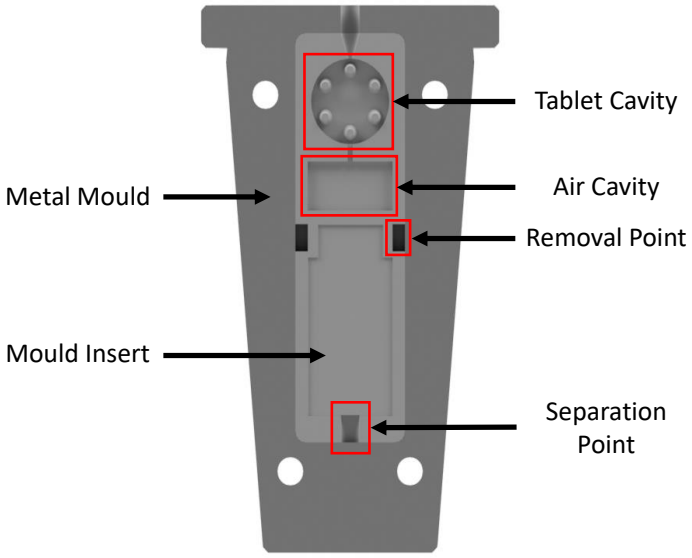

Figure 3: The mould insert for the 6 Pin Design inserted into the metal mould. This depiction represents one half of the full mould.

is an upright gas-pressurised injection moulder. The injection material is placed into the melt cylinder, the piston is attached and this is then placed into the injection moulder. A number of processing parameters must be set:

- Cylinder Temperature - *This is the temperature to which your injection material will be heated to.*
- Mould Temperature - *This is the temperature to which your mould will be heated to.*
- Injection Pressure - *This is the pressure which will be applied to the piston to move the injection material into the mould.*
- Injection Time - *This is the length of time for which your injection pressure will be applied.*
- Hold Pressure - *This is the pressure which will be applied after the injection material has filled the mould.*

- Hold Time - *This is the length of time for which your hold pressure will be applied.*

These processing parameters will vary for different injection materials. These are detailed in Table 4. The injection time, hold pressure and hold time for the formulations were kept constant at 10 s, 50 bar and 10 s respectively.

Table 4: RTIM process parameters used for each of the formulations. Formulations marked with * required the addition of a silicone based lubricant.

Formulation	**Cylinder Temp**	**Mould Temp**	**Injection Pressure**
AFF*	N/A	N/A	N/A
AFF/PEG 85/15*	200 °C	100 °C	150 bar
AFF/SA 85/15*	180 °C	100 °C	150 bar
AFF/PE 85/15*	180 °C	100 °C	150 bar
EPO/PEG 85/15*	N/A	N/A	N/A
KEF	140 °C	70 °C	150 bar
KELF	140 °C	70 °C	150 bar
KLF	140 °C	70 °C	150 bar
LDPE	150 °C	100 °C	150 bar
PVA*	200 °C	70 °C	200 bar
SOL/SOR 85/15*	N/A	N/A	N/A

A number of formulations also required the application of a silcone based lubricant onto the surface of the mould inserts to aid removal of the injected material. These formulations are marked with an * in the above table.

Three formulations were found to be unprocessable via this RTIM process namely AFF, EPO/PEG 85/15 and SOL/SOR 85/15. As such, no further data is presented on these formulations.

Upon completion of injection, the metal mould is removed from the injection moulder. The metal mould is then opened and the mould insert removed. When sufficiently cooled,

the mould insert is then opened and the tablet removed from the mould.

2.2.4. Gravimetric Analysis

All tablets produced were weighed on a 4 decimal point balance. The masses reported reflect the average of each batch produced. The mean and standard deviations reported are for $n = 20$ tablets (LDPE formulations) or $n = 6$ (all other formulations).

2.2.5. Dimensional Analysis

The width and height of each tablet was measured using digital callipers. A total of three diameter and three thickness measurements were taken for each tablet, the measurements shown are an average of these replicates. The mean and standard deviations reported are for $n = 20$ tablets (LDPE formulations) or $n = 6$ (all other formulations).

2.2.6. Optical Coherence Tomography

The technique used in this work features Spectral Domain Optical Coherence Tomography (OCT) and utilises the Thorlabs (GAN600 Series)(New Jersey, USA). This technique produces cross-sectional images of a sample which can be used for depth measurements. Measurements can be one-dimensional, two-dimensional or three-dimensional. For this work, two-dimensional measurements are used. The OCT is focused over the pins on the tablet surfaces. The focus is adjusted to ensure a strong signal. The diameters at both the top and bottom surfaces of the pins are measured as is the depth of each pin.

3. Results

3.1. Rapid Tooling Injection Moulding

3.2. Gravimetric Analysis

The mass of each tablet manufactured was recorded and the averages and standard deviations for each formulation are displayed in Figure 4a. No data is shown for the AFF, EPO/PEG 85/15 and SOL/SOR 85/15 formulations as they were unprocessable via this RTIM process.

The mass across the three designs should not vary significantly for any given formulation as the volume should be constant across all designs (this data can be found in

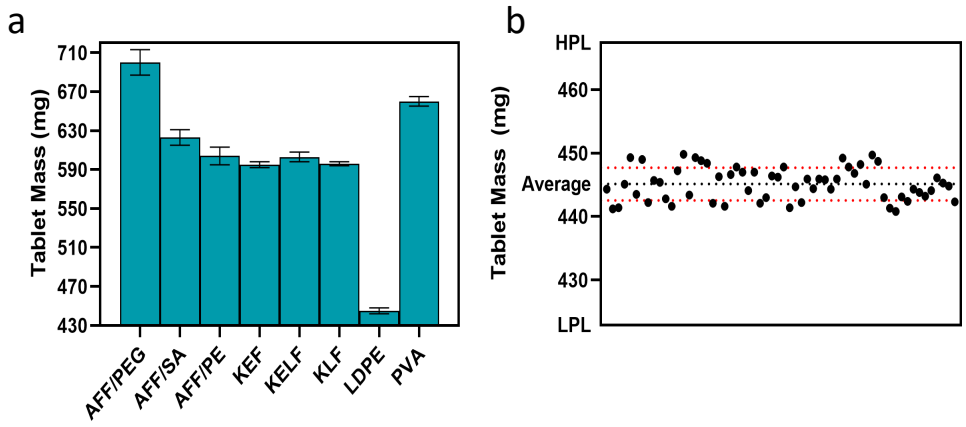

Figure 4: a) The average mass of all tablets for each formulation. Error bars represent the standard deviation ($n = 60$ for LDPE, $n = 18$ for all other formulations) b) The mass of 60 LDPE tablets (20 per design). The black dotted line represents the average tablet weight of this batch with the upper and lower red dotted lines being the average plus or minus the standard deviation respectively. HPL represents the higher pharmacopoeia limit (in this case taken as tablet weight +5%) and LPL is the lower pharmacopoeia limit (average tablet weight -5%).

Table S4 and Figure S1 in the supplementary information). The average mass does vary from one formulation to the next which is to be expected as the formulations will have different densities. The variation in mass observed across all formulations and all designs is well within the pharmacopoeia standards for tablet mass variation (The International Pharmacopoeia, 2019). Generally, a higher degree of variation was observed for the formulations which are Affinisol based. This is unsurprising as these formulations were difficult to process and the tablets produced had a tendency to stick to the mould surface if not removed while warm. This early removal from the mould could be responsible for the slightly reduced uniformity of mass compared with the other formulations tested.

Figure 4b demonstrates the tablet to tablet variability within the LDPE tablets. As all three designs should have equal mass, a total of 60 tablets are displayed here. The upper and lower limits on the y-axis represent the allowed deviation as per The International Pharmacopoeia limits of $\pm$ 5% (The International Pharmacopoeia, 2019).

From this we can clearly see that even within the larger batch size of 60 tablets, the mass variation is low and is well within the pharmacopoeia limits.

3.3. Dimensional Analysis

Both the tablet thickness and the tablet diameter (Figure 5) were measured. Figure **??**b shows the cylindrical structure of the tablets with the thickness represented by h_1 and the diameter represented by $2 \times r$. As above, no data is shown for the AFF, EPO/PEG 85/15 and SOL/SOR 85/15 formulations as they were unprocessable via this RTIM process. For all processable designs, the thickness of the tablets by design is constant at 3 mm. The diameter however is designed to increase moving from the 2 Pin through to 10 Pin designs. The designed diameter for the 2 Pin tablets is 15.231 mm, for the 6 Pin tablets is 15.684 mm and for the 10 Pin tablets is 16.124 mm.

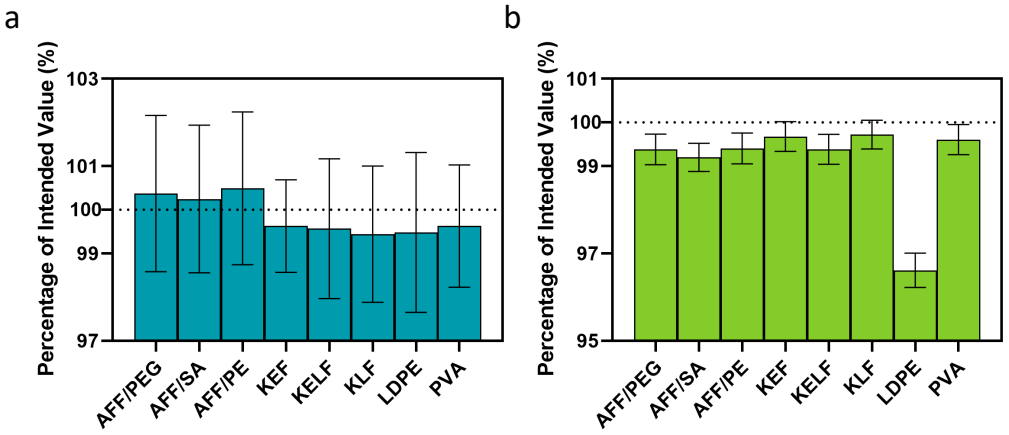

Figure 5: a) The thickness of the tablets tested for each geometry and formulation. For each bar, $n = 18$ measurements were taken and the error bars represent the standard deviation b) The diameter of the tablets tested for each geometry and formulation. For each bar, $n = 18$ measurements were taken and the error bars represent the standard deviation.

All formulations demonstrated good accuracy and precision to the digital designed thickness value of 3 mm. The AFF based formulations produced values slightly higher than the design value and the measurements had a higher standard deviation than the other formulations which is attributed to the difficulty associated with processing these formulations as previously discussed.

With the exception of LDPE, all formulations demonstrated good accuracy and precision to the digital designed diameter values across all three tablet geometries. The LDPE tablets were found to be consistently below the designed diameter values across all three

designs (ranging between 96.43 - 96.97% of the designed values). As polyethylene (and therefore LDPE) is a semi-crystalline thermoplastic, this can be attributed to shrinkage on cooling which is characteristic of crystalline polymers. While this was not observed to the same degree in the tablet thickness measurements where the LDPE tablets averaged 99.2% of the intended value, there was some evidence of the value being lower than anticipated and lower than all other formulations tested. Additionally, shrinkage is expected to be highest on the longest axis which for these designs would be the diameter.

3.4. Optical Coherence Tomography

The depth, top diameter and bottom diameter of the pins in all three geometries were measured using OCT. The depth is represented as h_2 in Figure **??**, the top diameter is $2 \times r_1$ and the bottom diameter is $2 \times r_2$. No data is shown for the AFF, EPO/PEG 85/15 and SOL/SOR 85/15 formulations as they were unprocessable via this RTIM process.

The depth of the pins (as seen in Figure 6a) was below the expected value of 2 mm across all formulations and geometries. While the measured values were consistently lower than expected, the low values of the standard deviations suggest that the variability within the batches was low.

The top diameter of the pins (as seen in Figure 6b) was generally above the expected value of 3 mm across all formulations and designs with the exception of the LDPE formulation. While the measured values were consistently higher than expected, the low values of the standard deviations suggest that the variability within the batches was low.

The bottom diameter of the pins (as seen in Figure 6c) was slightly below the expected value of 1.5 mm across all formulations and geometries. While the measured values were consistently slightly lower than expected, the low values of the standard deviations suggest that the variability within the batches was low.

4. Discussion

4.1. Formulation Processability in RTIM

Three of the formulations trialled were deemed to be unprocessable - AFF, EPO/PEG 85/15 and SOL/SOR 85/15. For the AFF formulation, the main challenge was around the temperatures and pressures required to process the material. The temperatures and

pressures required to achieve a workable viscosity of the formulation was too high for the mould materials to withstand causing fracture of the plastic mould inserts and ultimately resulting in an unsuccessful RTIM process. For EPO/PEG 85/15 and SOL/SOR 85/15, the issue with processing was down to the adherence of the formulation to the surface of the printed mould. While this is an issue that was encountered with a number of other formulations (those marked with * in Table 4), the addition of the silicon-based lubricant was not able to overcome the issues. For the EPO/PEG 85/15 and SOL/SOR 85/15 formulations a number of processing parameters were trialled including varying the temperatures for both the cylinder and the mould, reducing the injection pressure and the injection time. No successful processing conditions could be found for these materials in this specific RTIM process. The extent of the adhesion to the printed mould surface was such that the two mould halves were fused together. As such, removal of the tablets from these moulds was not possible and the formulations were deemed unprocessable.

4.2. Physical Parameters of the Tablets

From the dimensional analysis and the OCT analysis, the surface area, volume and specific surface area were calculated for the tablets produced. Full details of the equations used to calculate these parameters and the propagation of errors can be found in the supplementary information.

The average surface area, volume and specific surface area as calculated using Equations 3,4 and 5 are shown in Figures 7. The error bars shown are the product of error propagation using Equations 3, 4 and 5.

Theoretically, all formulations should produce physical parameters which match the digital design for their geometry. The digitally designed volume is constant across the three geometries, while the surface area and specific surface area increase with the increased number of pins.

There are a number of factors which create uncertainty in these calculated values. Primarily, there is an inherent uncertainty that arises from the printing of the plastic mould inserts. This is extensively studied in Walsh et al. (2021). Additionally, there are measurement errors associated with the different techniques used to measure the dimensions of the tablets. Finally, there will be errors associated with the different formulations used. This is most apparent when looking at the mass variability of the

formulations, where some have significantly higher standard deviations than others. The only variable changed in that case is the formulation so it can be assumed that the difference in standard deviation is attributed solely to the formulation differences.

I have calculated the measurement errors but not sure how to show that here.

A publication from Goyanes et al. found that the drug release kinetics were dependent on the specific surface area of the tablets (Goyanes et al., 2015). This is further supported by a later article by Martinez et al. which found the that the dissolution profile of a tablet could be fine-tuned by altering the specific surface area (Martinez et al., 2018). As such, in order to refine the dissolution to a desired profile, the control of the specific surface area must be accurate.

The average surface area of each of the tablets produced for each formulation is detailed in Figure 7a. From this it can be seen that for most formulations, the accuracy and precision of the surface area to the digital design is high. The exception to this is the LDPE formulation which, while still having high precision, has a much lower accuracy than the other formulations tested. It is proposed that this is due to the shrinkage on cooling associated with the crystalline nature of this polymer.

The average volume of each of the tablets produced for each formulation is detailed in Figure 7b. From this it can be seen that for most formulations, the accuracy and precision of the volume to the digital design is high. The exception to this is the LDPE formulation which, while still having high precision, has a much lower accuracy than the other formulations tested. As is also reflected in the surface area of the tablets from the LDPE formulation, the low accuracy for volume is attributed to the shrinkage of this polymer on cooling in the moulds.

The average specific surface area of each of the tablets produced for each formulation is detailed in Figure 7c. From this it can be seen that for all formulations, the accuracy and precision of the surface area to the digital design is high. As seen in Figures 7a and b, for the LDPE formulations the actual values fell below the intended values from the digital design. The drop in accuracy for both surface area and volume in the case of LDPE were so similar that the specific surface area is far more accurate to the digital design.

In summary, RTIM has proven to be an accurate and precise method for the produc-

tion of tablets with a desired specific surface area. This has been able to be modified through addition of pins into the tablet geometry and subsequent altering of the overall tablet diameter (see Figure 8).

4.3. Comparison to Similar Techniques

A number of publications have reported success in producing tablets via additive manufacture techniques such as fused deposition modelling (FDM) (Goyanes et al., 2014, 2015, 2016; Ibrahim et al., 2019; Goyanes et al., 2015) and stereolithography (SLA) (Martinez et al., 2018).

The relative standard deviation reported in Figure 9 demonstrates that the tablets produced using the RTIM method described in this work have a lower mass variability than other tablets produced via similar techniques (FDM or SLA). It is worth considering that the different manufacture techniques featured here are likely responsible for the differences in relative standard deviation. While both FDM and SLA are additive manufacture techniques and hence the tablets are built in a layer-by-layer process, the associated resolutions can be quite different. Typically, FDM has a lower resolution than SLA, ultimately resulting in a less accurate and precise printing process particularly for small features or objects. The RTIM process is formative, producing the tablets via a moulding using a mould created by SLA. As such, the actual formation of the tablet does not depend on a resolution limited additive manufacture process. These differences in manufacture process are also responsible for the differences in surface roughness that can be observed between tablets directly produced from FDM and those produced via RTIM. FDM tablets have significantly higher uncontrolled surface roughness. This surface roughness makes accuracy of surface area for tablets produced via FDM much harder to achieve and very difficult to accurately measure in the tablets produced.

As can be seen in Figure 10, the accuracy and precision of the PVA based tablets produced via RTIM were higher than that of the tablets produced via FDM. There are slight formulatory differences, with the PVA formulation used by Goyanes et al. containing approximately 4% w/w acetaminophen however it is not expected that this is responsible for the difference in accuracy and precision. The difference observed is likely due to the techniques involved in producing the tablets. FDM involves building the structure of the tablet on a layer by layer basis onto a build platform. There will be

limitations in terms of the accuracy of the print head in FDM and the geometry printed can also change as the printed material cools and solidifies. RTIM on the other hand produces the tablets via a fixed geometry mould cavity so the material is forced to adopt the desired geometry as it cools. This results in RTIM producing tablets which are truer to the digital design in terms of the physical properties than FDM. The precision of RTIM is also higher than the FDM process as can be seen by observing the error bars in Figure 10.

5. Conclusion

Tablets were able to be produced from a variety of thermoplastic materials and three tablet geometries were achieved. Generally, the tablets produced were close to the digital designs in terms of their dimensions, surface area and volume. Shrinkage upon cooling was observed for LDPE, a semi-crystalline polymer. In order to minimise the impact of shrinkage, a recommendation that amorphous formulations are most suitable for RTIM is made. The mass variability of all tablets produced was low and well within the limits of the pharmacopoeia. The tablets produced via RTIM demonstrated superior accuracy and precision in terms of physical properties to those produced directly via FDM. The specific surface areas of the tablets produced were accurate to the digital designs suggesting that this RTIM process could be used to produce tablets of designed geometries for the purpose of fine-tuning drug dissolution profiles.

Acknowledgements

The authors would like to thank EPSRC and the Future Continuous Manufacturing and Advanced Crystallisation Research Hub (Grant Ref EP/p00695/1), EPSRC (Grant Ref EP/N509760/1), Royal Society (Grant Ref RSG/R2/180276) and the University of Strathclyde for funding this research. The authors would like to acknowledge that this work was carried out in the CMAC National Facility supported by UKRPIF (UK Research Partnership Fund) award from the Higher Education Funding Council for England (HEFCE) (Grant Ref HH13054).

Declaration of Competing Interest

The authors declare that they have no known competing financial interests or personal relationships that could have appeared to influence the work reported in this paper.

References

A. Goyanes, P. Robles Martinez, A. Buanz, A. W. Basit, S. Gaisford, Effect of geometry on drug release from 3D printed tablets, International Journal of Pharmaceutics 494 (2015) 657–663. URL: http://dx.doi.org/10.1016/j.ijpharm.2015.04.069. doi:10.1016/j.ijpharm.2015.04.069.

M. Alomari, F. H. Mohamed, A. W. Basit, S. Gaisford, Personalised dosing: Printing a dose of one's own medicine, International Journal of Pharmaceutics 494 (2015) 568–577. URL: http://dx.doi.org/10.1016/j.ijpharm.2014.12.006. doi:10.1016/j.ijpharm.2014.12.006.

A. Goyanes, J. Wang, A. Buanz, R. Martínez-Pacheco, R. Telford, S. Gaisford, A. W. Basit, 3D Printing of Medicines: Engineering Novel Oral Devices with Unique Design and Drug Release Characteristics, Molecular Pharmaceutics 12 (2015) 4077–4084. doi:10.1021/acs.molpharmaceut.5b00510.

H. Y. Karasulu, G. Ertan, Different geometric shaped hydrogel theophylline tablets: Statistical approach for estimating drug release, Farmaco 57 (2002) 939–945. doi:10.1016/S0014-827X(02)01297-1.

J. Giboz, T. Copponnex, P. Mélé, Microinjection molding of thermoplastic polymers: A review, Journal of Micromechanics and Microengineering 17 (2007) 96–109. doi:10.1088/0960-1317/17/6/R02.

M. Heckele, W. K. Schomburg, Review on micro molding of thermoplastic polymers, Journal of Micromechanics and Microengineering 14 (2004). doi:10.1088/0960-1317/14/3/R01.

D. Annicchiarico, J. R. Alcock, Review of factors that affect shrinkage of molded part in injection molding, Materials and Manufacturing Processes (2014) 662–682. doi:10.1080/10426914.2014.880467.

L. Satin, J. Bílik, Impact of Viscosity on Filling the Injection Mould Cavity, Materials Science and Technology 24 (2016) 113–121.

N. Zhang, M. D. Gilchrist, Characterization of thermo-rheological behavior of polymer melts during the micro injection moulding process, Polymer Testing 31 (2012) 748–758. URL: http://dx.doi.org/10.1016/j.polymertesting.2012.04.012. doi:10.1016/j.polymertesting.2012.04.012.

I. Newton, Philosophiae naturalis principia mathematica, Jussu Societatis Regiae ac Typis Josephi Streater. Prostat apud plures bibliopolas, 1687. URL: https://library.si.edu/digital-library/book/philosophiaenat00newt. doi:10.5479/sil.52126.39088015628399.

S. Kashyap, D. Datta, Process parameter optimization of plastic injection molding: a review, International Journal of Plastics Technology (2015). doi:10.1007/s12588-015-9115-2.

G. Verstraete, J. Van Renterghem, P. J. Van Bockstal, S. Kasmi, B. G. De Geest, T. De Beer, J. P. Remon, C. Vervaet, Hydrophilic thermoplastic polyurethanes for the manufacturing of highly dosed oral sustained release matrices via hot melt extrusion and injection molding, International Journal of Pharmaceutics (2016). doi:10.1016/j.ijpharm.2016.04.057.

M. Packianather, C. Griffiths, W. Kadir, Micro injection moulding process parameter tuning, in: Procedia CIRP, 2015. doi:10.1016/j.procir.2015.06.093.

E. Walsh, J. H. ter Horst, D. Markl, Development of 3D Printed Rapid Tooling for Micro-Injection Moulding, Chemical Engineering Science (2021) 116498. URL: https://doi.org/10.1016/j.ces.2021.116498. doi:10.1016/j.ces.2021.116498.

The International Pharmacopoeia, 5.2 Uniformity of mass for single-dose preparations, World Health Organisation (2019) 1–2. URL: https://apps.who.int/phint/2019/index.html#p/home.

P. R. Martinez, A. Goyanes, A. W. Basit, S. Gaisford, Influence of Geometry on the Drug Release Profiles of Stereolithographic (SLA) 3D-Printed Tablets, AAPS PharmSciTech 19 (2018) 3355–3361. doi:10.1208/s12249-018-1075-3.

A. Goyanes, A. B. Buanz, A. W. Basit, S. Gaisford, Fused-filament 3D printing (3DP) for fabrication of tablets, International Journal of Pharmaceutics 476 (2014) 88–92. doi:10.1016/j.ijpharm.2014.09.044.

A. Goyanes, U. Det-Amornrat, J. Wang, A. W. Basit, S. Gaisford, 3D scanning and 3D printing as innovative technologies for fabricating personalized topical drug delivery systems, Journal of Controlled Release 234 (2016) 41–48. URL: http://dx.doi.org/10.1016/j.jconrel.2016.05.034. doi:10.1016/j.jconrel.2016.05.034.

M. Ibrahim, M. Barnes, R. McMillin, D. W. Cook, S. Smith, M. Halquist, D. Wijesinghe, T. D. Roper, 3D Printing of Metformin HCl PVA Tablets by Fused Deposition Modeling: Drug Loading, Tablet Design, and Dissolution Studies, AAPS PharmSciTech 20 (2019) 1–11. doi:10.1208/s12249-019-1400-5.

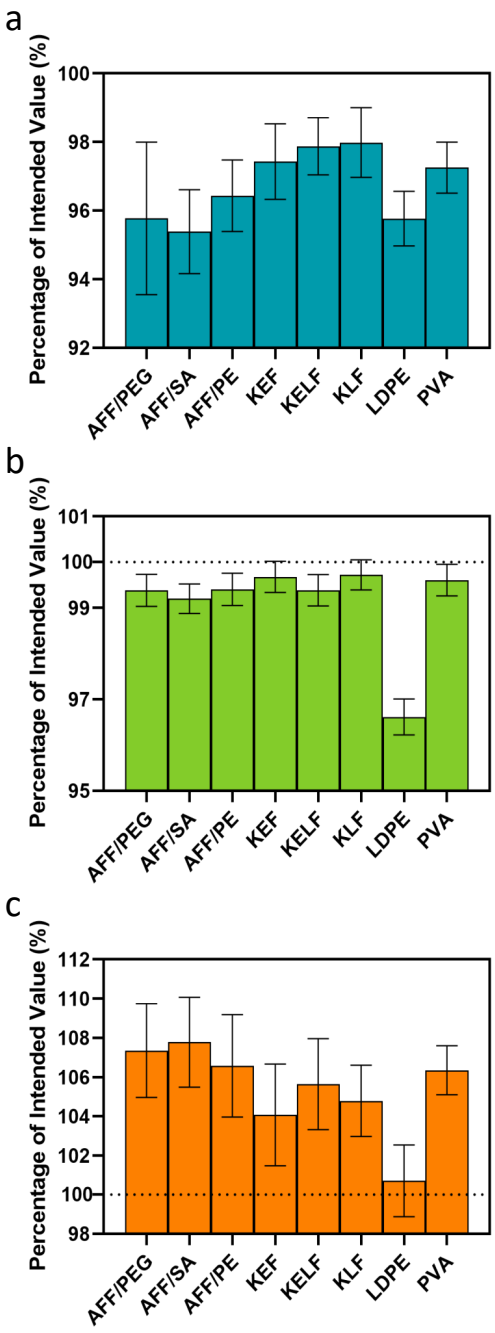

Figure 6: a) The depth of the pins on the tablet surface (h_2 from Figure **??**a)b) The top surface diameter of the pins on the tablet surface ($2 \times r_1$ from Figure **??**a) c) The bottom surface diameter of the pins on the tablet surface ($2 \times r_2$ from Figure **??**a). a-c: for each bar $n = 6$ measurements with the error bars representing the standard deviation.

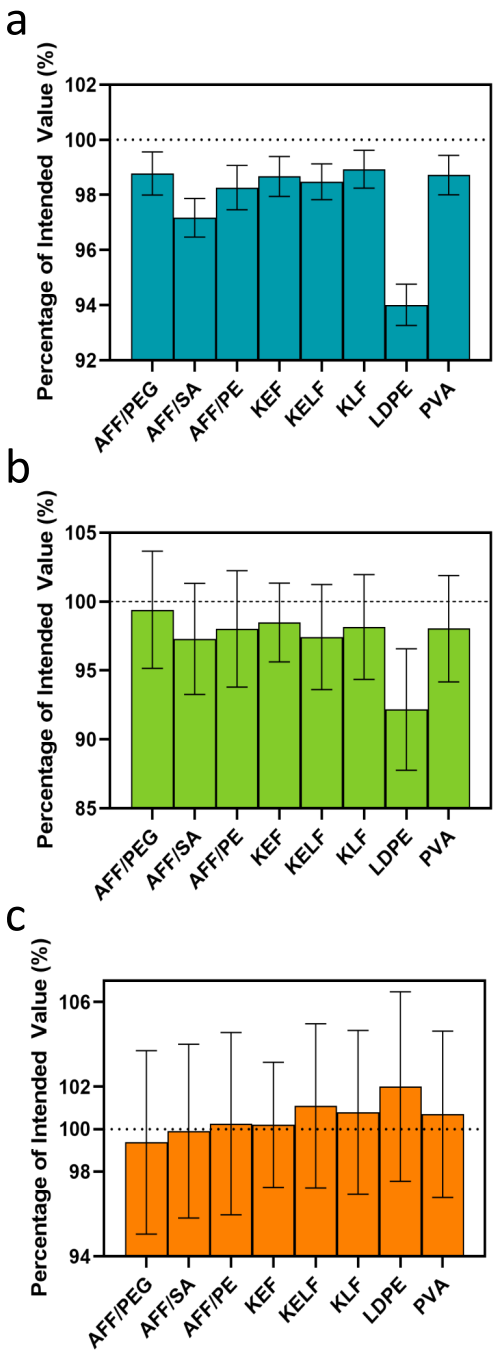

Figure 7: a) The average surface area for each formulation as calculated by Equation 3 b) The average volume for each formulation as calculated by Equation 4 c) The average specific surface area for each formulation as calculated by Equation 5. a-c: for each bar, $n = 18$ tablet with the error bars representing the propagated standard deviation.

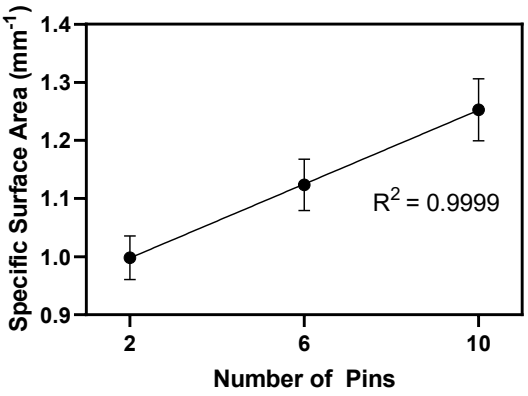

Figure 8: The average specific surface area for all formulations vs. the number of pins in the tablet geometry.

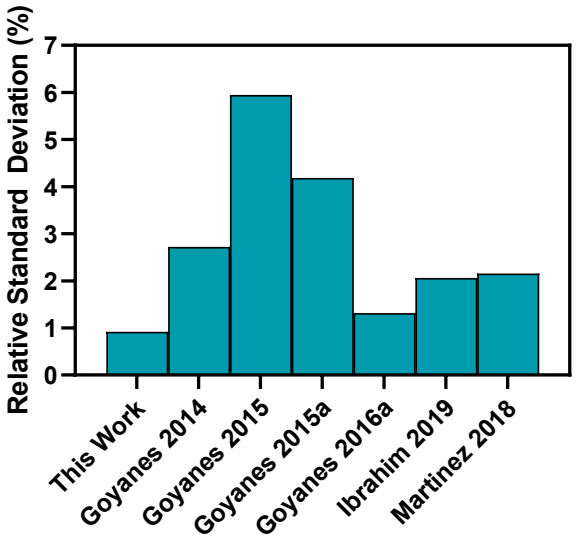

Figure 9: The relative standard deviation of tablet masses from this work and a number of similar manuscripts. From left to right, the manuscripts referenced are (Goyanes et al., 2014), (Goyanes et al., 2015), (Goyanes et al., 2015), (Goyanes et al., 2016), (Martinez et al., 2018) and (Ibrahim et al., 2019).

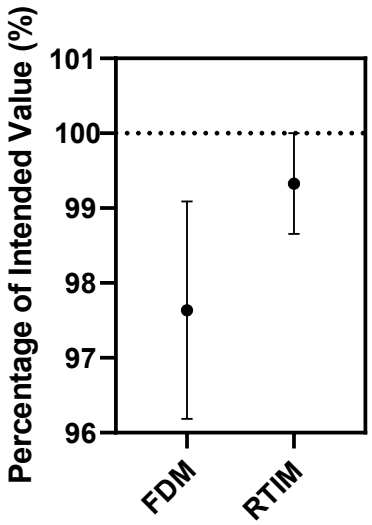

Figure 10: The percentage of the designed surface area of PVA based tablets from (Goyanes et al., 2015) and this study. The error bars represent the standard deviation for FDM and the propagated standard deviation for RTIM.